TRANSPORT OF THIOL-CONJUGATES OF INORGANIC MERCURY IN HUMAN RETINAL PIGMENT EPITHELIAL CELLS

Christy C. Bridges, **Jamie R. Battle**, and **Rudolfs K. Zalups**
Division of Basic Medical Sciences, Mercer University School of Medicine Macon, Georgia 31207

Abstract

Inorganic mercury (Hg^{2+}) is a prevalent environmental contaminant to which exposure to can damage rod photoreceptor cells and compromise scotopic vision. The retinal pigment epithelium (RPE) likely plays a role in the ocular toxicity associated with Hg^{2+} exposure in that it mediates transport of substances to the photoreceptor cells. In order for Hg^{2+} to access photoreceptor cells, it must be first be taken up by the RPE, possibly by mechanisms involving transporters of essential nutrients. In other epithelia, Hg^{2+}, when conjugated to cysteine (Cys) or homocysteine (Hcy), gains access to the intracellular compartment of the target cells via amino acid and organic anion transporters. Accordingly, the purpose of the current study was to test the hypothesis that Cys and Hcy *S*-conjugates of Hg^{2+} utilize amino acid transporters to gain access into RPE cells. Time- and temperature-dependence, saturation kinetics, and substrate-specificity of the transport of Hg^{2+}, was assessed in ARPE-19 cells exposed to the following *S*-conjugates of Hg^{2+}: Cys (Cys-*S*-Hg-*S*-Cys), Hcy (Hcy-*S*-Hg-*S*-Hcy), *N*-acetylcysteine (NAC-*S*-Hg-*S*-NAC) or glutathione (GSH-*S*-Hg-*S*-GSH). We discovered that only Cys-*S*-Hg-*S*-Cys and Hcy-*S*-Hg-*S*-Hcy were taken up by these cells. This transport was Na^+-dependent and was inhibited by neutral and cationic amino acids. RT-PCR analyses identified systems $B^{0,+}$ and ASC in ARPE-19 cells. Overall, our data suggest that Cys-*S*-Hg-*S*-Cys and Hcy-*S*-Hg-*S*-Hcy are taken up into ARPE-19 cells by Na-dependent amino acid transporters, possibly systems $B^{0,+}$ and ASC. These amino acid transporters may play a role in the retinal toxicity observed following exposure to mercury.

Keywords

retinal pigment epithelium; transport; inorganic mercury; amino acid transporters

INTRODUCTION

Mercury can exist in the environment in three different forms: elemental (Hg^0), inorganic (Hg^{2+}) and organic (primarily as methylmercury; CH_3Hg^+). Hg^0 and Hg^{2+} are released into the environment from the emissions of coal-burning plants and mining processes. Some of the released Hg^{2+} is biotransformed by microbial methylation to form CH_3Hg^+, which humans are exposed to via the consumption of contaminated water and/or food (ATSDR, 2003). Over 90′ of ingested CH_3Hg^+ is absorbed by the gastrointestinal tract (Kershaw et al., 1980). After

being $^+$ is oxidized to Hg^{2+}, either in plasma or within target absorbed, an appreciable fraction of CH_3Hg cells, (Dunn and Clarkson, 1980;Gage, 1964;Norseth and Clarkson, 1970a,b;Omata et al., 1980). Similarly, Hg^0 entering systemic circulation can also undergo oxidation to form Hg^{2+} (Engqvist et al., 1998;Magos et al., 1989;Ogata and Aikoh, 1983;Sichak et al., 1986). Since cellular exposure to Hg^{2+} can be detrimental, it is important to determine how mercuric ions are handled by target cells that are affected adversely by this metal.

Exposure of certain organs and cells to Hg^{2+} can result in serious toxicological consequences, including cell death. One such organ is the eye. The visual system has been shown to be susceptible to the toxicological effects of mercuric ions. *In vivo* studies in laboratory animals have shown that vision loss can result after exposure to Hg^0, CH_3Hg^+ or Hg^{2+}, (ATSDR, 2003;Evans and Garman, 1980;Finocchio et al., 1980;Fox and Sillman, 1979;Shaw et al., 1980;Tessier-Lavigne et al., 1985;Warfvinge and Bruun, 1996). Indeed, one of the earliest signs of mercury poisoning is an impairment of scotopic (night) vision (Evans and Garman, 1980). This aspect of vision is mediated primarily by rod photoreceptor cells, which are unable to respond appropriately to light following exposure to mercuric compounds (Evans and Garman, 1980;Tessier-Lavigne, 1985). In addition, chronic exposure to mercury may result in a perturbation of peripheral vision, followed by a more severe loss of central vision (Evans and Garman, 1980;Finocchio et al., 1980;Saldana et al., 2006). Surprisingly, the actual mechanisms by which mercuric ions gain access to the photoreceptor cells and cause subsequent vision loss are unclear.

In order for mercury to gain access to photoreceptor cells, it must first cross the retinal pigment epithelium (RPE). The RPE is a single layer of epithelial cells positioned strategically between the choriocapillaris and the neural retina. Specifically, the basolateral plasma membrane is apposed to the choroidal capillaries while the apical microvilli interdigitate with the outer segments of photoreceptor cells. Because of this location, the RPE is responsible for the transport of nutrients and wastes to and from the photoreceptor cells. Owing to tight junctions between cells, the movement of substances across the RPE is mediated mainly by specific protein transporters present on the basolateral and apical plasma membranes. Interestingly, the membrane localization of certain proteins in the RPE is opposite that of most epithelia (Bok, 1993;Chancy et al., 2000;Marmorstein, 2001;Smith et al., 1999). This unique distribution is important in maintaining the basolateral to apical flow of nutrients across the RPE. In addition to essential nutrients and ions, the RPE may also deliver toxic compounds and metals such as lead, cadmium, and mercury to the photoreceptors. Indeed, following exposure to Hg^0, mercuric ions have been detected in the RPE and photoreceptor cells (Warfvinge and Bruun, 1996). This accumulation can have significant detrimental effects on the RPE and the adjacent photoreceptors (Erie et al., 2005;Fox and Sillman, 1979;Tessier-Lavigne et al., 1985;Warfvinge and Bruun, 1996,2000).

The mechanisms by which mercuric ions are taken up into and exported out of RPE cells remain unclear. In other epithelia, Hg^{2+} and CH_3Hg^+, as *S*-conjugates of thiol-containing molecules, have been shown to gain access to intracellular compartments of cells through the actions of amino acid and/or organic anion transporters (Clarkson, 1993;Bridges and Zalups, 2005). Mercuric ions bind readily to the reduced sulfur atom of thiol-containing molecules, such as cysteine (Cys), homocysteine (Hcy), and glutathione (GSH) to form thermodynamically stable linear II coordinate covalent complexes (Fuhr and Rabenstein, 1973). The Cys and Hcy conjugates of Hg^{2+} (Cys-*S*-Hg-*S*-Cys and Hcy-*S*-Hg-*S*-Hcy, respectively) are similar structurally to cystine and homocystine. Therefore, we hypothesized that these complexes are taken up at the site of one or more transporters of cystine and/or homocystine. Indeed, studies in Madin-Darby canine kidney (MDCK) cells indicate that the luminal uptake of Cys-*S*-Hg-*S*-Cys and Hcy-*S*-Hg-*S*-Hcy in proximal tubular cells is mediated by the amino acid transporter, system $b^{0,+}$ (Bridges et al., 2004;Bridges and Zalups, 2004). System $b^{0,+}$ is the principal

sodium-independent transporter of cystine on the luminal plasma membrane of proximal tubular cells, which are the primary cellular targets that take up and are affected adversely by Hg^{2+}.

Inasmuch as humans continue to be exposed to CH_3Hg^+, Hg^0 and Hg^{2+} and, since this exposure can result in visual impairment, the purpose of the current study was to identify mechanisms in RPE that may play a role in the delivery of mercuric ions to photoreceptor cells. Considering that CH_3Hg^+ and Hg^0 oxidize to form Hg^{2+} within the body, the primary focus of this study was to examine the handling of Hg^{2+}. Initially, we tested the hypothesis that amino acid carriers play a role in the transport of Cys-*S*-Hg-*S*-Cys and Hcy-*S*-Hg-*S*-Hcy across the RPE. Indeed, analyses of time- and temperature-dependence, saturation kinetics and substrate-specificity of the transport of Cys-*S*-Hg-*S*-Cys and Hcy-*S*-Hg-*S*-Hcy provide indirect evidence supporting the theory that these two conjugates are transported by one or more Na^+-dependent amino acid transporters present in the plasma membrane of RPE cells.

MATERIALS AND METHODS

Tissue Culture

ARPE-19 cells (American Type Culture Collection, Manassas, VA) are an immortalized line of human RPE cells that accurately reflect RPE cells *in vivo* (Dunn et al., 1996,1998). Cells were cultured in Dulbecco's modified Eagle's medium/Ham's F-12 50/50 mixture (Mediatech, Herndon, VA) supplemented with 10′ fetal bovine serum (Atlanta Biologicals, Atlanta, GA), 100 U/ml penicillin, and 100 μg/ml streptomyocin (Invitrogen, Carlsbad, CA). Cells were sub-cultured by incubation in 0.25′ trypsin (Invitrogen) in phosphate buffered saline (PBS) containing 0.5 mM ethylenediaminetetraacetic acid (EDTA). Prior to experimentation, cells were seeded at 0.3×10^6 cells per well in 24-well plates and cultured for 24 h to obtain confluent monolayers. Cultures were maintained at 37° C in a humidified atmosphere of 5′ CO_2 and 95′ O_2.

Reverse-transcriptase Polymerase Chain Reaction Analyses of Transporter Expression

RT-PCR analyses were carried out in order to confirm the presence of RNA encoding $ATB^{0,+}$ and ASC2 in ARPE-19 cells. It is assumed that the presence of RNA encoding these two transporters is indicative of the expression of the $ATB^{0,+}$ and ASC2 proteins.

Total RNA was isolated from the cells using TRIzol Reagent (Invitrogen) according to the manufacturer's instructions. RT-PCR analyses were performed using the Gene Amp kit from Applied Biosystems (Foster City, CA). The presence of $ATB^{0,+}$ and ASC2 was assayed using primers specific to each transporter to yield 425- and 405-base-pair fragments, respectively. The primers for each transporter are as follows: $ATB^{0,+}$, 5'-CGT GCC CGG CCC ATT CTA AG-3' and 5'AAA ACC ACC ATT GAG CAC CCT ACA-3'; ASC2, 5'-GGG GCA GGA GGT GGA GGG GAT GA-3' and 5'-AGC GTG GCG GAA CTG GAA GAG GTC-3'. For both sets of primers, the PCR conditions were as follows: 94°C, 30s; 57°C, 30s; 72°C, 1 min for 35 cycles. RT-PCR products were electrophoresed on a 0.8′ agarose gel stained with ethidium bromide.

Evaluation of Transport

Uptake experiments using ARPE-19 cells were carried out as described previously (Bridges et al., 2001a,b;Naggar et al., 2003). At the beginning of each experiment, culture medium was removed and cells were washed with warm (37°C) uptake buffer (25 mM Hepes, 140 mM NaCl, 5.4 mM KCl, 1.8 mM $CaCl_2$, 0.8 mM $MgSO_4$, 5 mM glucose, pH 7.5/Tris). In some experiments, NaCl was replaced with 140 mM *N*-methyl-D-glucamine (NMDG) in order to determine the role of Na^+ in the uptake of specific mercuric species. Cells were incubated with

250 μL of an individual mercuric conjugate for 30 min at 37°C, unless otherwise noted. At the end of the incubation, the radiolabeled substances were aspirated from the culture dishes and the remaining cells were washed twice with cold (4°C) uptake buffer containing 1 mM sodium 2,3-dimercaptopropane-1-sulfonate (DMPS; Sigma, Saint Louis, MO), a well-known chelator of mercuric ions (Aposhian, 1983;Ruprecht, 1997). After the final washes had been completed, cells were solubilized with 1′ SDS in 0.2 N NaOH and the suspension was added to a scintillation vial containing 5 mL of Optifluor scintillation fluid (Perkin Elmer, Boston, MA). The radioactivity of each sample was determined by liquid scintillation spectrometry using a Beckman LS6500 scintillation counter (Beckman, Fullerton, CA)

Mercuric conjugates of Cys, Hcy, glutathione (GSH) and N-acetylcysteine (NAC) were generated by mixing 5 μM $HgCl_2$, containing [$^{203}Hg^{2+}$], with 12.5 μM of the respective thiol. This mixture was allowed to incubate at room temperature for at least 5 min. The $^{203}Hg^{2+}$ (2.36 mCi/mg) was generated by neutron activation of ^{202}HgO at the Missouri University Research Reactor (Aslamkhan et al., 2003;Belanger et al., 2001).

In order to determine the species of Hg^{2+} taken up by RPE cells, uptake of Hg^{2+} was measured as a conjugate of one of several common thiol-containing biomolecules. Cells were incubated with $^{203}Hg^{2+}$, as a conjugate of Cys (Cys-S-Hg-S-Cys), Hcy (Hcy-S-Hg-S-Hcy), GSH (GSH-S-Hg-S-GHS), or NAC (NAC-S-Hg-S-NAC) in the presence NaCl or NMDG for 30 min at 37°C or 4°C.

The effects of time and temperature on the transport of Cys-S-Hg-S-Cys or Hcy-S-Hg-S-Hcy were evaluated by measuring the Na^+-dependent and independent uptake of each conjugate at 37°C and 4°C for times ranging from 5 to 60 min. Experiments designed to measure the saturation kinetics for the transport of Cys-S-Hg-S-Cys or Hcy-S-Hg-S-Hcy were performed by incubating cells with Cys-S-[^{203}Hg]-S-Cys or Hcy-S-[^{203}Hg]-S-Hcy for 30 min at 37°C or 4°C in the presence of unlabeled Cys-S-Hg-S-Cys or Hcy-S-Hg-S-Hcy (0.5, 1, 5, 10, 25, 50, 75, or 100 μM). These experiments were carried out in the presence and absence of Na^+. Substrate-specificity analyses were carried out by incubating cells with Cys-S-[^{203}Hg]-S-Cys or Hcy-S-[^{203}Hg]-S-Hcy in the presence of one of the following unlabeled amino acids: methionine, cysteine, leucine, phenylalanine, isoleucine, alanine, arginine, lysine, serine, glycine, homocysteine, glutamate, aspartate, N-methylaminoisobutyric acid (MeAIB); or the organic anion, para-aminohippurate (PAH). These compounds were chosen based on their charge and utilization by specific amino acid transporters. MeAIB and PAH are classic inhibitors of system A and the organic anion transporter (OAT1 and OAT3), respectively. System A has not been identified as a mechanism for the transport of mercuric compounds (Cannon et al., 2001) while OAT has been shown to transport several conjugates of Hg^{2+} and $CH_3Hg^{+,}$ (Aslamkhan et al., 2003;Zalups and Ahmad, 2004,2005a,2005b). In addition, some cells were exposed to Cys-S-[^{203}Hg]-S-Cys or Hcy-S-[^{203}Hg]-S-Hcy in the presence of a combination of two unlabeled amino acids (methionine and lysine, methionine and cysteine, methionine and arginine, alanine and cysteine, arginine and cysteine, or lysine and cysteine). In these experiments, all amino acids were used at a concentration of 3 mM and all experiments were carried out in the presence and absence of NaCl.

Moreover, the transport of Cys-S-Hg-S-Cys or Hcy-S-Hg-S-Hcy was also measured in the presence of increasing concentrations of cystine or homocystine, respectively. Cells were exposed to 5 μM Cys-S-[^{203}Hg]-S-Cys or Hcy-S-[^{203}Hg]-S-Hcy in the presence of unlabeled cystine or homocystine (0, 25, 50, 75, 100, 250, 500, or 750 μM). Alternatively, cells were incubated with 5 μM [^{35}S]-cystine (0.6 mCi/mg; Amersham, Piscataway, NJ) in the presence of unlabeled Cys-S-Hg-S-Cys (0, 5, 10, 25, 50, 100, 250, or 500 μM). These experiments were all carried out in the presence of NaCl. The uptake of radiolabeled homocystine in the presence

of unlabeled Hcy-*S*-Hg-*S*-Hcy was not examined due to the unavailability of a radiolabeled form of homocystine.

Assessment of Cellular Viability

The toxicological effects of $HgCl_2$, Cys-*S*-Hg-*S*-Cys, Hcy-*S*-Hg-*S*-Hcy, and GSH-*S*-Hg-*S*-GSH on ARPE-19 cells were measured using a methylthiazoletetrazolium (MTT) assay, as described previously (Bridges et al., 2004;Bridges and Zalups, 2004). ARPE-19 cells were seeded at a density of 0.3×10^6 cells/mL in 96-well culture dishes (200 μL/well). After growing to confluence (24 h), cells were washed twice with warm, uptake buffer containing NaCl and were then treated with $HgCl_2$, Cys-*S*-Hg-*S*-Cys, Hcy-*S*-Hg-*S*-Hcy, or GSH-*S*-Hg-*S*-GSH (0, 5, 25, 50, 100 or 250 μM). The cells were incubated for 30 min at 37°C in a humidified atmosphere of 5′ CO_2. Cells were then washed twice with cold (4°C) uptake buffer and incubated with 0.5 mg/ml MTT for 2 h at 37°C, in a humidified atmosphere of 5′ CO_2. After this incubation, 100 μL of solubilization buffer (10′ Triton X-100 and 0.1 N HCl in isopropyl alcohol) were added to each well and the mixture was allowed to incubate for 16 h at room temperature. Each plate was read at 490 nm in a BioTek μQuant spectrophotometric plate reader (BioTek, Winooski, VT).

Data Analyses

All experiments were performed at least twice with triplicate measurements for each condition. Data for each parameter assessed were analyzed first with the Kolmogorov-Smirnov test for normality and then with Levene's test for homogeneity of variance. The corresponding means for each set of data were subsequently compared using a one- or two-way analysis of variance (ANOVA). When significant F-values were obtained, differences among means were assessed using Tukey's multiple-comparison procedure. A *p* value of <0.05 was considered statistically significant.

RESULTS

Uptake of Mercuric Conjugates of Thiol-Containing Biological Molecules

Uptake of Hg^{2+}, as Cys-*S*-Hg-*S*-Cys, Hcy-*S*-Hg-*S*-Hcy, GSH-*S*-Hg-*S*-GSH, or NAC-*S*-Hg-*S*-NAC was measured in the cells in the presence of NaCl or NMDG at either 37°C or 4°C (Figure 1). Uptake of Cys-*S*-Hg-*S*-Cys at 37°C was approximately threefold greater in the presence of NaCl than in the presence of NMDG. Similarly, the inward transport of Hcy-*S*-Hg-*S*-Hcy at 37°C was more than twofold greater under Na^+-dependent conditions compared with that under Na^+-independent conditions. Interestingly, significant differences were also noted between the Na^+-dependent and Na^+-independent transport of GSH-*S*-Hg-*S*-GSH, as well as that of NAC-*S*-Hg-*S*-NAC.

Under Na^+-dependent conditions, uptake of Cys-*S*-Hg-*S*-Cys or Hcy-*S*-Hg-*S*-Hcy at 37°C was approximately threefold greater than that in cells exposed to GSH-*S*-Hg-*S*-GSH or NAC-*S*-Hg-*S*-NAC at 37°C. When cells were exposed to Cys-*S*-Hg-*S*-Cys, Hcy-*S*-Hg-*S*-Hcy, GSH-*S*-Hg-*S*-GSH, or NAC-*S*-Hg-*S*-NAC at 4°C in the presence of NMDG or NaCl, the uptake of Hg^{2+} was relatively similar among all groups.

Uptake of Hg^2+ as Cys-S-Hg-S-Cys or Hcy-S-Hg-S-Hcy

Time-course analyses for the Na^+-dependent and independent uptake of Cys-*S*-Hg-*S*-Cys (Figure 2A) or Hcy-*S*-Hg-*S*-Hcy (Figure 2B) in ARPE-19 cells were carried out at 4°C and 37°C. These data show that, at 37°C, the rates of uptake of either conjugate increased significantly over 60 min of exposure. At nearly every time studied, the uptake of Cys-*S*-Hg-*S*-Cys and Hcy-*S*-Hg-*S*-Hcy in the presence of NaCl was significantly greater at 37°C than at

4°C. Furthermore, the uptake of these conjugates at 37°C in Na^+-dependent conditions was also significantly greater than uptake of these conjugates in the presence of NMDG at either 4°C or 37°C.

The saturation kinetics of Cys-*S*-Hg-*S*-Cys or Hcy-*S*-Hg-*S*-Hcy transport were studied and compared in the presence of NaCl or NMDG at 37°C and 4°C. At 37°C, the overall rate of uptake of Cys-*S*-Hg-*S*-Cys (Figure 3A) was significantly greater in the presence of NaCl than in the presence of NMDG. At 4°C, there was no difference in the amount of Hg^{2+} associated with cells exposed to either NaCl or NMDG. Using the Michaelis-Menten equation, the maximal velocity (V_{max}) for the Na^+-dependent uptake of Cys-*S*-Hg-*S*-Cys at 37°C was calculated to be 111 ± 29.5 pmol x mg protein^{-1} x min^{-1} while the Michaelis-Menten constant (K_m) was 160 ± 62.4 μM. These values were calculated by subtracting the uptake of Cys-*S*-Hg-*S*-Cys in the presence of NaCl at 37°C from the uptake of Cys-*S*-Hg-*S*-Cys in the presence of NMDG at 37°C. In order to distinguish among the activities of individual transporters, kinetic data obtained under Na^+-dependent and independent conditions at 37°C were plotted by the Eadie-Hofstee method (Figure 4A). The data points representing Na^+-dependent transport were obtained by subtracting the NMDG data from the NaCl data. Based on these plots, it appears that there are at least two distinct, Na^+-dependent, transport processes responsible for the uptake of Cys-*S*-Hg-*S*-Cys. There also appear to be two processes involved in the Na^+-independent uptake of Cys-*S*-Hg-*S*-Cys, although this uptake represents a minor component of Cys-*S*-Hg-*S*-Cys entry.

Analysis of saturation kinetics for the transport of Hcy-*S*-Hg-*S*-Hcy (Figure 3B), revealed that the uptake of this conjugate at 37°C in the presence of NaCl (as compared to NMDG) was significantly greater at every concentration of Hcy-*S*-Hg-*S*-Hcy examined. The V_{max} for this uptake was calculated to be 84.6 ± 12.8 pmol x mg protein^{-1} x min^{-1}, while the K_m was 78.3 ± 21.9 μM. These values were obtained by subtracting the Na^+-dependent uptake of Hcy-*S*-Hg-*S*-Hcy from the corresponding Na^+-dependent uptake. The amount of Hg^{2+} associated with cells exposed to NaCl at 4°C was not significantly different from that of cells exposed to NMDG. Data obtained under Na^+-dependent and independent conditions at 37°C were then plotted using the Eadie-Hofstee method in order to differentiate among individual transport processes (Figure 4B). As before, in order to more accurately represent Na^+-dependent transport, NMDG data was subtracted from the NaCl data. Like that of Cys-*S*-Hg-*S*-Cys, the Na^+-dependent transport of Hcy-*S*-Hg-*S*-Hcy also appears to occur via two distinct processes.

Substrate-specificity for the transport of Cys-*S*-Hg-*S*-Cys (Figure 5A) or Hcy-*S*-Hg-*S*-Hcy (Figure 6A) in the presence and absence of Na^+ was also assessed. Uptake of either of these conjugates in the presence of Na^+ was significantly reduced by the addition of the following unlabeled neutral or cationic amino acids: methionine, cysteine, leucine, phenylalanine, isoleucine, alanine, arginine, lysine, serine, glycine, and homocysteine. Interestingly, exposure to the anionic amino acid, glutamate, also diminished uptake of each conjugate, although exposure to aspartate, which is also anionic, did not. Neither MeAIB (a substrate of system A) nor PAH (a substrate of OAT1 and OAT3) inhibited significantly the uptake of Cys-*S*-Hg-*S*-Cys or Hcy-*S*-Hg-*S*-Hcy. In the absence of Na^+, only cysteine significantly inhibited the uptake of Cys-*S*-Hg-*S*-Cys, while the uptake of Hcy-*S*-Hg-*S*-Hcy was inhibited by methionine, cysteine, arginine, serine, and homocysteine.

In separate experiments, cells were exposed to Cys-*S*-Hg-*S*-Cys (Figure 5B) or Hcy-*S*-Hg-*S*-Hcy (Figure 6B) in the presence of either a single amino acid or a combination of two amino acids. In the presence of Na^+, the addition of methionine and cysteine, alanine and cysteine, arginine and cysteine, or lysine and cysteine reduced the transport of Cys-*S*-Hg-*S*-Cys and Hcy-*S*-Hg-*S*-Hcy, in an additive manner, to levels significantly lower than those measured when these conjugates were exposed to a single amino acid. In the absence of Na^+, there was little

difference in the uptake of Cys-*S*-Hg-*S*-Cys among groups of cells. The Na^{+}-independent uptake of Hcy-*S*-Hg-*S*-Hcy was significantly lower than control levels when cells were exposed to the following combinations: methionine and cysteine, methionine and arginine, arginine and cysteine, lysine and cysteine.

The effect of unlabeled cystine or homocystine on the uptake of Cys-*S*-Hg-*S*-Cys (Figure 7A) and Hcy-*S*-Hg-*S*-Hcy (Figure 8), respectively, was also measured in ARPE-19 cells. Surprisingly, the uptake of each conjugate increased over time as the concentration of corresponding disulfide was increased. Alternatively, when the uptake of radiolabeled cystine was analyzed in the presence of unlabeled Cys-*S*-Hg-*S*-Cys, the uptake of cystine was diminished significantly in a concentration-dependent manner (Figure 7B).

Cellular Viability Assays

Cellular viability of ARPE-19 cells was assessed following the exposure to different species of Hg^{2+} was evaluated to determine the relationship between cellular transport of Hg^{2+} and intoxication (Figure 9). After a 30-min exposure to 250 μM Cys-*S*-Hg-*S*-Cys or GSH-*S*-Hg-*S*-GSH, there was no significant reduction in the viability of ARPE-19 cells. In contrast, exposure to 250 μM Hcy-*S*-Hg-*S*-Hcy decreased cellular viability by about 18′. Exposure to HgCl$_2$ was used as a positive control since it has been demonstrated to induce a substantial degree of cell death in cultured MDCK cells (Bridges et al., 2004). Cellular viability in ARPE-19 cells declined by approximately 18′ following exposure to 5 μM HgCl$_2$. Finally, after exposure to 250 μM HgCl$_2$, cellular viability decreased by about 65′.

RT-PCR Analyses of Amino Acid Transporters in ARPE-19 cells

The presence of mRNA transcripts encoding systems B[0,+] and ASC in ARPE-19 cells was examined using RT-PCR (Figure 10). RT-PCR products of the expected sizes were obtained for both of these transport systems.

DISCUSSION

Since exposure to various forms of mercury can impair vision, it is important to understand the manner in which mercuric ions gain access to photoreceptor cells. These cells do not have a direct blood supply, but obtain all nutrients from the choroid via vectorial transport across the RPE. Although the transport of numerous substances across this cell-layer has been characterized, the mechanisms by which toxic compounds, such as metal complexes, cross the RPE are not yet understood. Therefore, the purpose of the current study was to test the hypothesis that transportable mercuric species, such as Cys-*S*-Hg-*S*-Cys and Hcy-*S*-Hg-*S*-Hcy, are taken up by ARPE-19 cells via amino acid transporters present in the plasma membrane. The results of the current study suggest that ARPE-19 cells are indeed capable of transporting Cys-*S*-Hg-*S*-Cys and Hcy-*S*-Hg-*S*-Hcy and that this transport is mediated, at least in part, by Na^{+}-dependent amino acid transporters.

The ability of RPE cells to transport Cys-*S*-Hg-*S*-Cys, Hcy-*S*-Hg-*S*-Hcy, GSH-*S*-Hg-*S*-GSH, or NAC-*S*-Hg-*S*-NAC was examined in the current study. Of these conjugates, only Cys-*S*-Hg-*S*-Cys and Hcy-*S*-Hg-*S*-Hcy appear to be taken up by ARPE-19 cells. Similarly, these two conjugates have been identified as transportable forms of Hg^{2+} in other cell-types (Aslamkhan et al., 2003;Bridges et al., 2004;Bridges and Zalups, 2004;Zalups and Ahmad, 2004;Zalups et al., 2004). Moreover, the majority of the transport of these conjugates by RPE cells appears to require the presence of Na^{+}. In contrast, the uptake of GSH-*S*-Hg-*S*-GSH and NAC-*S*-Hg-*S*-NAC was significantly lower than that of Cys-*S*-Hg-*S*-Cys or Hcy-*S*-Hg-*S*-Hcy. This finding was not surprising since GSH-*S*-Hg-*S*-GSH and NAC-*S*-Hg-*S*-NAC are large and/or negatively

charged at physiologic pH and have not been shown to be taken up by amino acid transporters in other types of cells.

To characterize the uptake of Cys-*S*-Hg-*S*-Cys or Hcy-*S*-Hg-*S*-Hcy in ARPE-19 cells, analyses of temperature- and time-dependence of this transport were carried out in the presence and absence of NaCl. The uptake of either conjugate was significantly greater at 37°C than that at 4°C, which suggests that the transport of Cys-*S*-Hg-*S*-Cys and Hcy-*S*-Hg-*S*-Hcy in ARPE-19 cells is mediated by carrier proteins. Also, a small fraction of this transport appears to be due to Na^+-independent mechanisms. In addition, the transport of each conjugate increased over time at 37°C, although this transport did not appear to reach a plateau during the times studied. This lack of plateau may have been related to the intracellular bonding characteristics of Hg^{2+}. Once Hg^{2+} gains access to the intracellular environment, it can move freely from one thiol to another and can bind readily to any thiol-containing molecule, including low-molecular-weight and protein thiols present within the cytoplasm and organelles. Therefore, once Hg^{2+} has gained access to the intracellular compartment of ARPE-19 cells, it may release the thiol (i.e. Cys or Hcy) to which it is bound in order to bond with other, more prevalent, free thiols. Cys and Hcy may then be utilized by the cell or oxidized to cystine or homocystine, respectively, and be transported back out into the extracellular space. Since these two disulfide amino acids are removed from the cell, the negative feedback loop that would halt their inward transport is not invoked. This may, therefore, result in the continued deposition of mercuric ions, via the uptake Cys-*S*-Hg-*S*-Cys and Hcy-*S*-Hg-*S*-Hcy, into the intracellular space of the cell.

Analyses of saturation kinetics for the transport of Cys-*S*-Hg-*S*-Cys and Hcy-*S*-Hg-*S*-Hcy suggested that the uptake of these two conjugates occurs primarily by a Na^+-dependent, carrier-mediated process. Based on Eadie-Hofstee analyses, we can conclude that there are at least two distinct transport mechanisms responsible for the Na^+-dependent transport of each conjugate. Possible carriers involved in this transport include, but are not limited to, organic anion transporters (OAT), which are indirectly dependent upon Na^+ for their activity, and amino acid transporters, such as systems $B^{0,+}$, ASC, or A (Ganapathy et al., 2004;Kekuda et al., 1996;Sloan and Mager 1999). Interestingly, uptake of Cys-*S*-Hg-*S*-Cys and Hcy-*S*-Hg-*S*-Hcy did not appear to plateau, even at a concentration of 100 μM, indicating a lack of transporter saturation. This may be related to the low affinity of the transporter(s) for each conjugate or the presence of multiple transport proteins involved in the uptake of these compounds. These transporters likely become saturated only after exposure to much higher concentrations of Cys-*S*-Hg-*S*-Cys or Hcy-*S*-Hg-*S*-Hcy. In the present study, however, ARPE-19 cells were not exposed to either conjugate at concentrations greater than 100 μM because of observed decreases in cellular viability (Figure 9). Interestingly, plasma levels of Hg^{2+} in humans following acute exposure mercury vapor have been found to be as high as 293 μM (Houeto et al., 1994). Because of the lack of transporter saturation at 100 μM, it is likely that these carriers may contribute to mercury intoxication by their continual uptake of Hg^{2+}.

Substrate specificity experiments were carried out in order to determine a possible mechanism (s) for the transport of Cys-*S*-Hg-*S*-Cys or Hcy-*S*-Hg-*S*-Hcy into RPE cells. Not surprisingly, the presence of various neutral and positively charged amino acids inhibited the Na^+-dependent uptake of Cys-*S*-Hg-*S*-Cys or Hcy-*S*-Hg-*S*-Hcy into RPE cells, indicating that amino acid transporters are responsible for at least a fraction of this uptake. Since MeAIB did not affect significantly the transport of Cys-*S*-Hg-*S*-Cys or Hcy-*S*-Hg-*S*-Hcy, it can be concluded that system A does not play a role in this process. This conclusion is further supported by findings from isolated perfused rabbit proximal tubules where system A was ruled out as a carrier of Cys-*S*-Hg-*S*-Cys (Cannon et al., 2001). More likely candidates for this transport include systems $B^{0,+}$ and ASC. Indeed, RNA encoding these amino acid transport systems was identified in ARPE-19 cells (Figure 10). System $B^{0,+}$ transports cationic amino acids in addition

to cysteine and other neutral amino acids (Sloan and Mager, 1999). Given that the cationic amino acids, lysine and arginine, significantly inhibited the uptake of Cys-*S*-Hg-*S*-Cys or Hcy-*S*-Hg-*S*-Hcy in the ARPE-19 cells, it seems probable that system $B^{0,+}$ is involved in this transport. Similarly, system ASC has been shown to transport alanine, serine, cysteine, and glutamate (Kekuda et al., 1996;Palacin et al., 1998). Since all of these amino acids had an inhibitory effect on the uptake of Cys-*S*-Hg-*S*-Cys or Hcy-*S*-Hg-*S*-Hcy, one is led to believe that system ASC is also involved in the uptake of either mercuric species. Taken together, our data tend to indirectly implicate systems $B^{\circ,+}$ and ASC in the uptake of Cys-*S*-Hg-*S*-Cys and Hcy-*S*-Hg-*S*-Hcy.

When the Na^+-independent uptake of Cys-*S*-Hg-*S*-Cys was measured in the presence of various amino acids, we found that the uptake of this conjguate was inhibited significantly by cysteine, suggesting that a small fraction of this uptake is due to a Na^+-independent transporter. Furthermore, when the uptake of Hcy-*S*-Hg-*S*-Hcy was measured in the presence of various amino acids, we found that several neutral amino acids and a cationic amino acid, arginine, were able to inhibit the uptake of this conjugate. These data also suggest that there may be a small Na^+-independent component of Hg^{2+} transport in RPE cells.

In a separate experiment, the Na^+-dependent uptake of either Cys-*S*-Hg-*S*-Cys or Hcy-*S*-Hg-*S*-Hcy was measured in the presence of cysteine and a second amino acid. The uptake of either mercuric conjugate was reduced to levels significantly lower than those measured in the presence of each amino acid individually. These data suggest that one of the carriers responsible for the uptake of these conjugates has a high affinity for cysteine, as well as for neutral amino acids (e.g. system ASC), while another transporter (e.g. system $B^{0,+}$) is less specific and prefers neutral and cationic amino acids. Interestingly, the presence of excess cystine or homocystine stimulated the uptake of Cys-*S*-Hg-*S*-Cys or Hcy-*S*-Hg-*S*-Hcy, respectively. This stimulation is likely due to a trans-stimulatory effect in which cystine or homocystine within the cell is exchanged for Cys-*S*-Hg-*S*-Cys and Hcy-*S*-Hg-*S*-Hcy, respectively. Indeed this effect has been shown to occur with these conjugates at the sites of other transport proteins (Bridges et al., 2004;Bridges and Zalups, 2004).

In summary, the data from the current study provide indirect evidence suggesting that Cys-*S*-Hg-*S*-Cys and Hcy-*S*-Hg-*S*-Hcy are transported by RPE cells, possibly via the amino acid transporters systems $B^{0,+}$ and ASC. Although additional studies are clearly needed to characterize more accurately the roles of individual transport proteins in the handling of Cys-*S*-Hg-*S*-Cys or Hcy-*S*-Hg-*S*-Hcy by the RPE, the findings from the present study are important to human health in that they identify possible mechanisms that may play a role in allowing Hg^{2+} to access photoreceptor cells of the neural retina, where subsequent damage may occur.

References

Agency for Toxic Substance and Disease Registry. Toxicological profile for mercury. US Department of Health and Human Services, Public Health Service, Centers for Disease Control; Atlanta, GA: 2003.

Aposhian HV. DMSA and DMPS – water soluble antidotes for heavy metal poisoning. Ann Rev Pharmacol Toxicol 1983;23:193–215. [PubMed: 6307120]

Aslamkhan AG, Han YH, Yang XP, Zalups RK, Pritchard JB. Human renal organic anion transporter 1-dependent uptake and toxicity of mercuric-thiol conjugates in Madin-Darby Canine Kidney cells. Mol Pharmacol 2003;63:590–596. [PubMed: 12606766]

Belanger M, Westin A, Barfuss DW. Some health physics aspects of working with ^{203}Hg in university research. Health Phys 2001;80(Suppl 1):S28–S30. [PubMed: 11197511]

Bok D. The retinal pigment epithelium: a versatile partner in vision. J Cell Sci 1993;17(Suppl):189–195.

Bridges CC, Bauch C, Verrey F, Zalups RK. Mercuric conjugates of cysteine are transported by the amino acid transporter system b$^{0,+}$: Implications of molecular mimicry. J Am Soc Nephrol 2004;15:663–673. [PubMed: 14978168]

Bridges CC, Kekuda R, Prasad PD, Mehta P, Huang W, Smith SB, Ganapathy V. Structure, function, and regulation of human cystine/glutamate transporter in retinal pigment epithelial cells. Invest Ophthalmol Vis Sci 2001a;42:47–54. [PubMed: 11133847]

Bridges CC, Ola MS, Prasad PD, El-Sherbeny A, Ganapathy V, Smith SB. Regulation of taurine transporter expression by NO cultured human retinal pigment epithelial cells. Am J Physiol Cell Physiol 2001b;281:C1825–C1836. [PubMed: 11698241]

Bridges CC, Zalups RK. Homocysteine, system b$^{0,+}$ and the renal epithelial transport and toxicity of inorganic mercury. Am J Pathol 2004;165:1385–1394. [PubMed: 15466402]

Bridges CC, Zalups RK. Molecular and ionic mimicry and the transport of toxic metals. Toxicol Appl Pharmacol 2005;204:274–308. [PubMed: 15845419]

Cannon VT, Zalups RK, Barfuss DW. Amino acid transporters involved in luminal transport of mercuric conjugates of cysteine in rabbit proximal tubule. J Pharmacol Exp Therap 2001;298:780–789. [PubMed: 11454942]

Chancy CD, Kekuda R, Huang W, Prasad PD, Kuhnel JM, Sirotnak FM, Roon P, Ganapathy V, Smith SB. Expression and differential polarization of the reduced- folate transporter-1 and the folate receptor α in mammalian retinal pigment epithelium. J Biol Chem 2000;275:20676–20684. [PubMed: 10787414]

Clarkson TW. Molecular and ionic mimicry of toxic metals. Ann Rev Biochem 1993;32:545–571.

Dunn KC, Aotaki-Keen AE, Putkey FR, Hjelmeland LM. ARPE-19, A human retinal pigment epithelial cell line with differentiated properties. Exp Eye Res 1996;62:155–169. [PubMed: 8698076]

Dunn JD, Clarkson TW. Does mercury exhalation signal demethylation of methylmercury? Health Physiol 1980;38:477–414.

Dunn KC, Marmorstein AD, Bonilha VL, Rodriquez-Boulan E, Giordano F, Hjelmeland LM. Use of the ARPE-19 cell line as a model of RPE polarity: Basolateral secretion of FGF5. Invest Ophthalmol Vis Sci 1998;39:2744–2749. [PubMed: 9856785]

Engqvist A, Colmsjo A, Skare I. Speciation of mercury excreted in feces from individuals with amalgam fillings. Arch Environ Health 1998;53:205–213. [PubMed: 9814717]

Erie JC, Butz JA, Good JA, Erie EA, Burritt MF, Cameron JD. Heavy metal concentrations in human eyes. Am J Ophthalmol 2005;139:888–893. [PubMed: 15860295]

Evans, HL.; Garman, RH. Scotopic vision as an indicator of neurotoxicity. In: Merigan, WH.; Weiss, B., editors. Neurotoxicity of the Visual System. New York: Raven Press; 1980. p. 135-147.

Finocchio, DV.; Luschei, ES.; Mottet, NK.; Body, R. Effects of methylmercury on the visual system of rhesus macaque (*Macaca Mulatta*). I. Pharmacokinetics of chronic methylmercury related to changes in vision and behavior. In: Merigan, WH.; Weiss, B., editors. Neurotoxicity of the Visual System. New York: Raven Press; 1980. p. 113-122.

Fox DA, Sillman AJ. Heavy metals affect rod, but not cone, photoreceptors. Science 1979;206:78–80. [PubMed: 314667]

Fuhr B, Rabenstein DL. Nuclear magnetic resonance studies of the solution chemistry of metal complexes. IX. The binding of cadmium, zinc, lead, and mercury by glutathione. J Am Chem Soc 1973;95:6944–6950. [PubMed: 4784285]

Gage JC. Distribution and excretion of methyl and phenylmercury salts. Br J Ind Med 1964;21:197–202. [PubMed: 14180477]

Ganapathy, V.; Inoue, K.; Prasad, PD.; Ganapathy, ME. In Metabolic and Therapeutic Aspects of Amino Acids in Clinical Nutrition. Boca Raton, FL: CRC Press; 2004. Cellular uptake of amino acids: systems and regulation; p. 63-78.

Houeto P, Sandouk P, Baud FJ, Levillain P. Elemental mercury vapour toxicity: Treatment and levels in plasma and urine. Human Exp Toxicol 1994;13:848–852.

Kekuda T, Prasad PD, Fei YJ, Torres-Zamorano V, Sinha S, Yang-Feng TL, Leibach FH, Ganapathy V. Cloning of the sodium-dependent, broad-scope, neutral amino acid transporter B^0 from a human placental choriocarcinoma cell line. J Biol Chem 1996;271:18657–18661. [PubMed: 8702519]

Kershaw TG, Clarkson TW, Dhahir P. The relationship between blood levels and dose of methylmercury in man. Arch Environ Health 1980;35:28–36. [PubMed: 7189107]

Magos L, Clarkson TW, Hudson AR. The effects of dose of elemental mercury and first-pass circulation time on exhalation and organ distribution of inorganic mercury in rats. Biochim Biophys Acta 1989;991:85–89. [PubMed: 2713425]

Marmorstein AD. The polarity of the retinal pigment epithelium. Traffic 2001;2:867–872. [PubMed: 11737824]

Naggar H, Fei YJ, Ganapathy V, Smith SB. Regulation of reduced-folate transporter-1 (RFT-1) by homocysteine and identity of transport systems for homocysteine uptake in retinal pigment epithelial (RPE) cells. Exp Eye Res 2003;77:687–697. [PubMed: 14609557]

Norseth T, Clarkson TW. Studies on the biotransformation of ^{203}Hg-labeled methylmercury chloride in rats. Arch Environ Health 1970a;21:717–727. [PubMed: 5478557]

Norseth T, Clarkson TW. Biotransformation of methylmercury salts in the rat studied by specific determination of inorganic mercury. Biochem Pharmacol 1970b;19:2775–2783. [PubMed: 5478586]

Ogata M, Aikoh H. The oxidation mechanism of metallic mercury in vitro by catalase. Physiol Chem Phys Med NMR 1983;15:89–91. [PubMed: 6647575]

Omata S, Sata M, Sakimura K, Sugano H. Time-dependent accumulation of inorganic mercury in subcellular fractions of kidney, liver, and brain or rats exposed to methylmercury. Arch Toxicol 1980;44:231–241. [PubMed: 7396710]

Palacin M, Estevez R, Bertran J, Zorzano A. Molecular biology of mammalian plasma membrane amino acid transporters. Physiol Rev 1998;78:969–1054. [PubMed: 9790568]

Ruprecht, J. Scientific Monograph Dimaval (DMPS). Heyltex Corp; Houston, TX: 1997.

Saldana M, Collins CE, Gale R, Backhouse O. Diet-related mercury poisoning resulting in visual loss. British J Ophthalmol 2006;90:1432–1434.

Shaw, CM.; Mottet, NK.; Chen, WJ. Effects of methylmercury on the visual system of rhesus macaque (*Macaca Mulatta*). II. Neuropathological findings (with emphasis on vascular lesions in the brain). In: Merigan, WH.; Weiss, B., editors. Neurotoxicity of the Visual System. New York: Raven Press; 1980. p. 123-134.

Sichak SP, Mavis RD, Finkelstein JN, Clarkson TW. An examination of the oxidation of mercury vapor by rat brain homogenate. J Biochem Toxicol 1986;1:53–68. [PubMed: 3271871]

Sloan JL, Mager S. Cloning and functional expression of a human Na^+ and Cl^--dependent neutral and cationic amino acid transporter $B^{0,+}$ J Biol Chem 1999;274:23740–23745. [PubMed: 10446133]

Smith SB, Kekuda R, Gu X, Chancy C, Conway SJ, Ganapathy V. Expression of folate receptor α in the mammalian retinal pigment epithelium. Invest Ophthalmol Vis Sci 1999;40:840–848. [PubMed: 10102280]

Tessier-Lavigne M, Mobbs P, Attwell D. Lead and mercury toxicity and the rod light response. Invest Ophthalmol Vis Sci 1985;26:1117–1123. [PubMed: 2991162]

Warfvinge K, Bruun A. Mercury accumulation in the Squirrel monkey eye after mercury varpour exposure. Toxicol 1996;107:189–200.

Warfvinge K, Bruun A. Mercury distribution in the squirrel monkey retinal after *in utero* exposure to mercury vapor. Environ Res 2000;83:102–109. [PubMed: 10856182]

Zalups RK, Ahmad S. Homocysteine and the renal epithelial transport and toxicity of inorganic mercury: role of basolateral transporter organic anion transporter 1. J Am Soc Nephrol 2004;15:2023–2031. [PubMed: 15284288]

Zalups RK, Ahmad S. Handling of the homocysteine S-conjugate of methylmercury by renal epithelial cells: role of organic anion transporter 1 and amino acid transporters. J Pharmacol Exp Ther 2005a; 315:896–904. [PubMed: 16081680]

Zalups RK, Ahmad S. Transport of N-acetylcysteine s-conjugates of methylmercury in Madin-Darby canine kidney cells stably transfected with human isoform of organic anion transporter 1. J Pharmacol Exp Therap 2005b;314:1158–1168. [PubMed: 15908511]

Zalups RK, Aslamkhan AG, Ahmad S. Human organic anion transporter 1 mediates cellular uptake of cysteine-*S*-conjugates of inorganic mercury. Kidney Int 2004;66:251–261. [PubMed: 15200431]
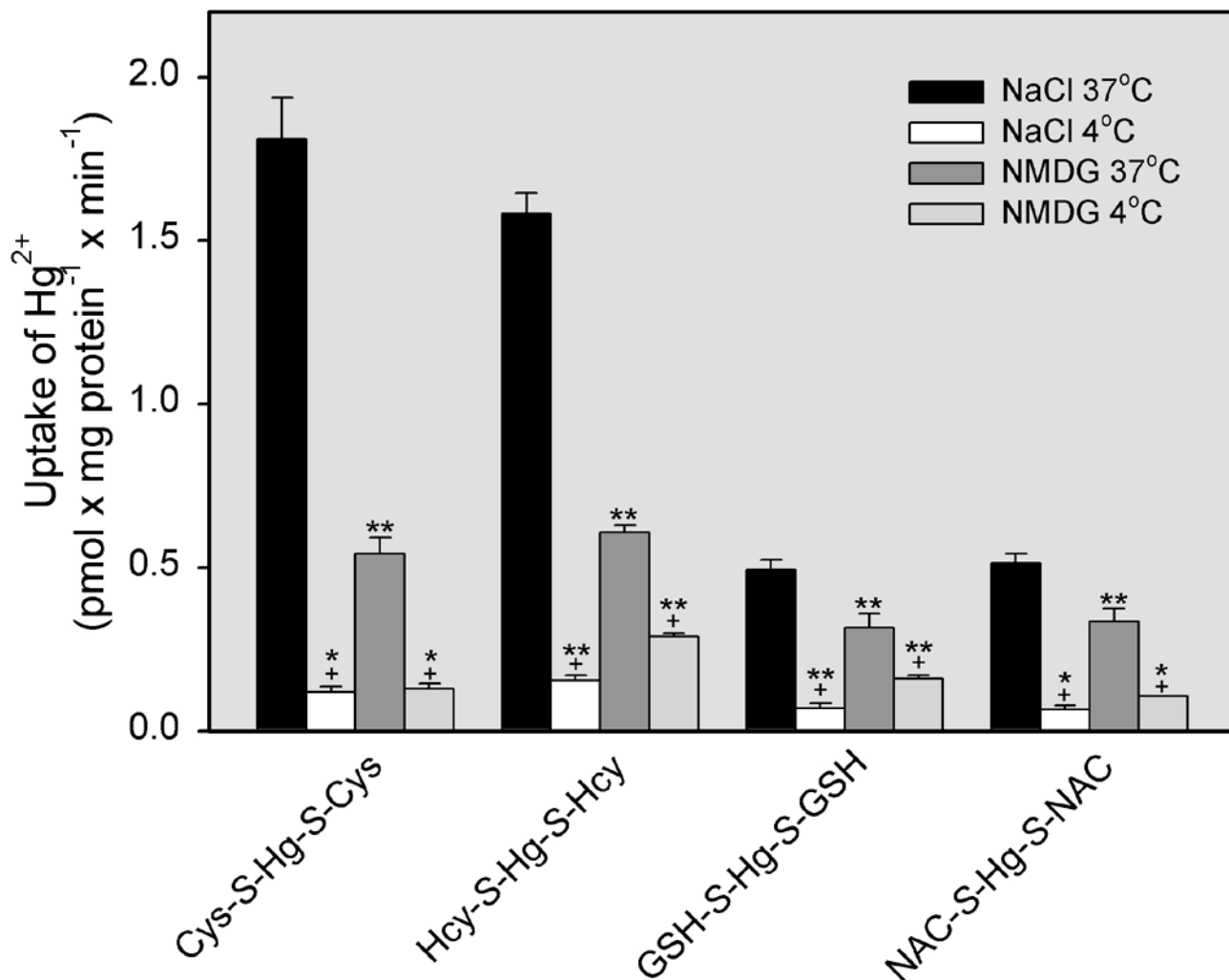
Figure 1.
Uptake of inorganic mercury (Hg^{2+}) as a conjugate of cysteine (Cys-*S*-Hg-*S*-Cys), homocysteine (Hcy-*S*-Hg-*S*-Hcy), glutathione (GSH-*S*-Hg-*S*-GSH), or N-acetylcysteine (NAC-*S*-Hg-*S*-NAC) in ARPE-19 cells. Cells were exposed to one of these conjugates (5 μM) for 30 min at 37°C in the presence of NaCl or N-methyl-D-glucamine (NMDG). Results are presented as means ± standard error. Data represent two experiments performed in quadruplicate. *, significantly different (p < 0.05) from the mean for the corresponding group of cells (exposed to the same conjugate) in the presence of NaCl or NMDG at 37°C. **, significantly different (p < 0.05) from the means of all other corresponding groups of cells. +, significantly (p < 0.05) from the mean of the corresponding groups of cells exposed to the same buffer.
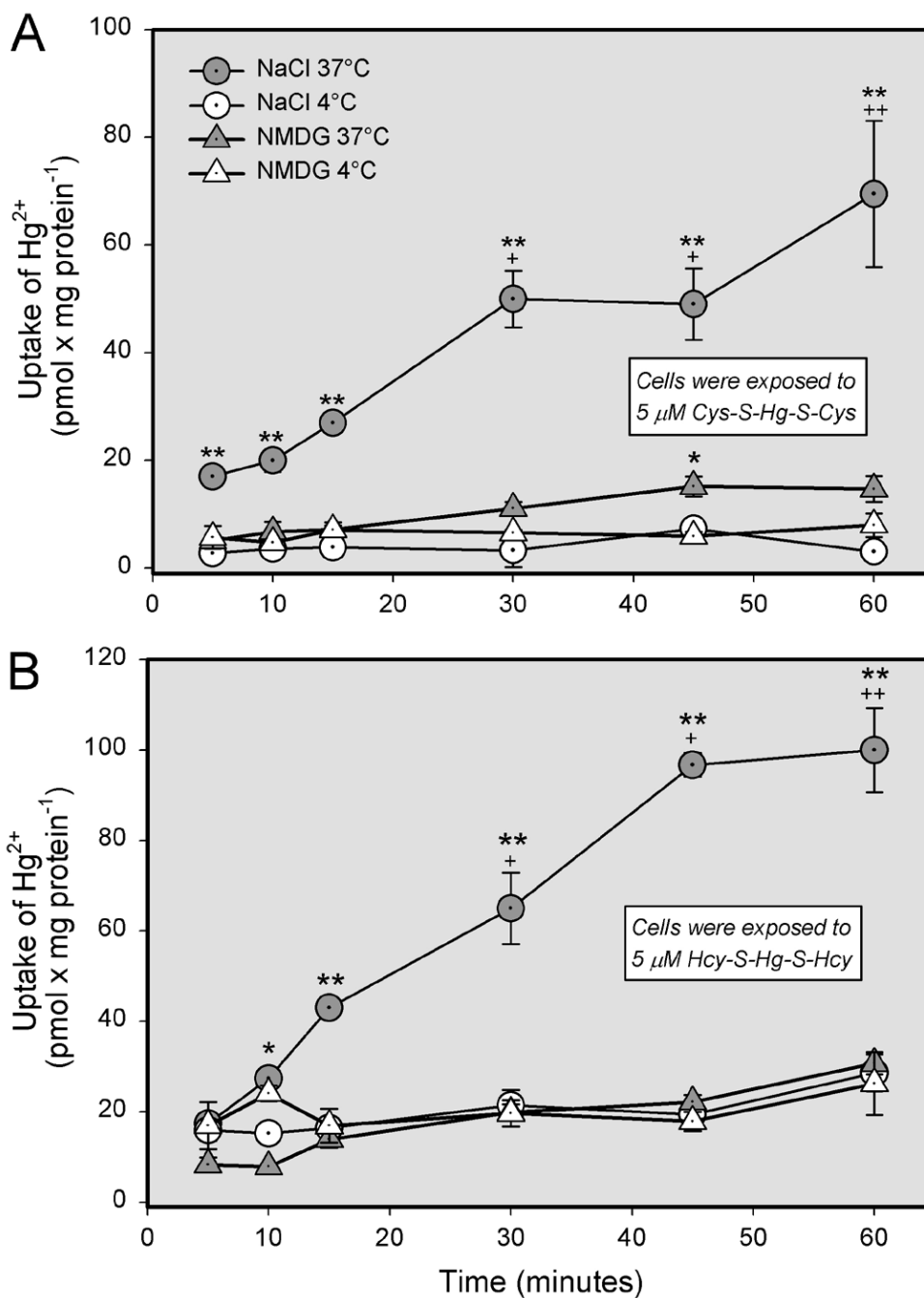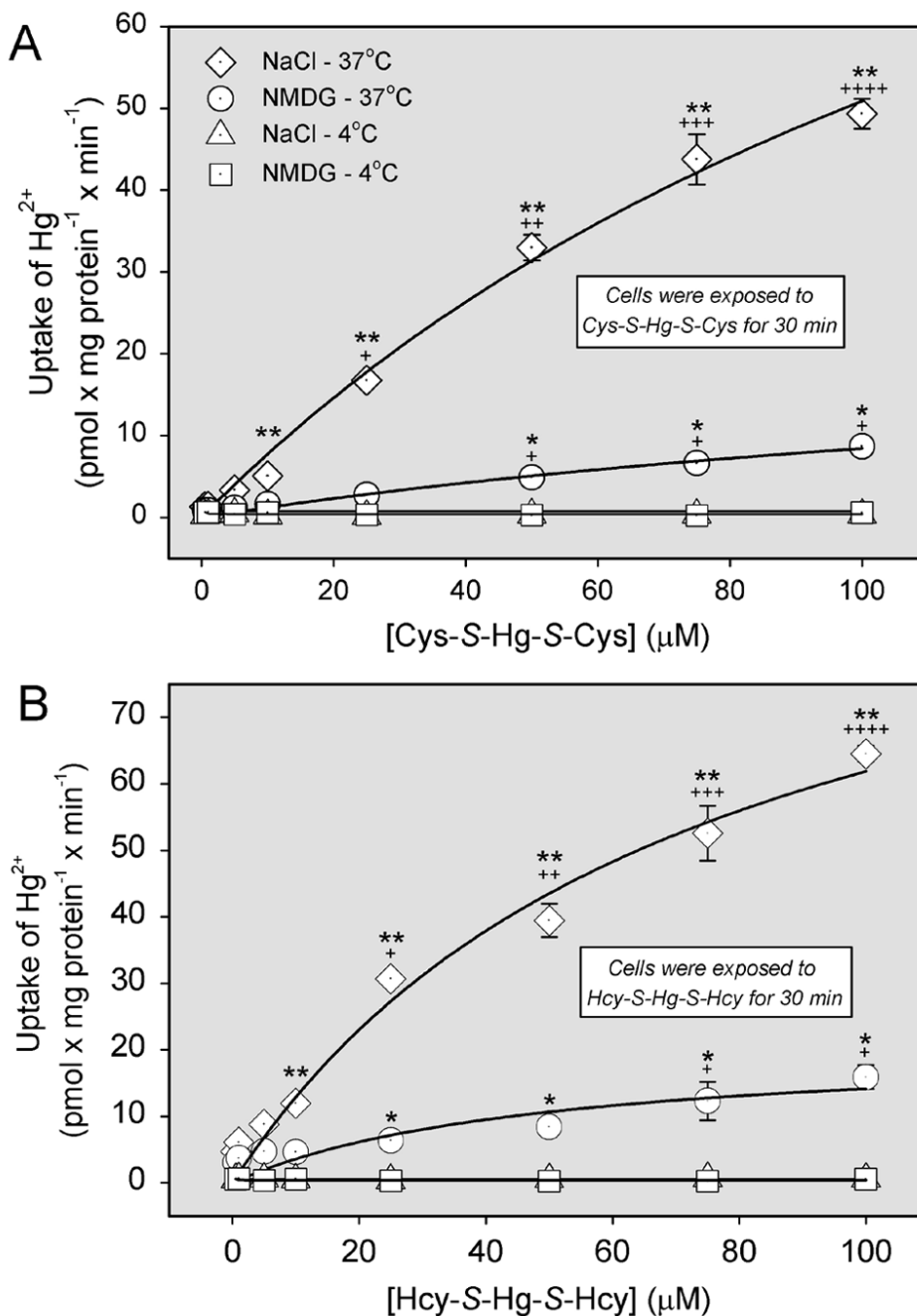
Figure 2.
Time- and temperature-dependence of the transport of inorganic mercury (Hg^{2+}) as a conjugate of cysteine (Cys-*S*-Hg-*S*-Cys) or homocysteine (Hcy-*S*-Hg-*S*-Hcy) in ARPE-19 cells. Cells were exposed to 5 μM Cys-*S*-Hg-*S*-Cys (A) or Hcy-*S*-Hg-*S*-Hcy (B) in the presence of NaCl for various times at either 4°C or 37°C. Results are presented as means ± standard error. Data represent two experiments performed in triplicate. *, significantly different ($p < 0.05$) from the mean for the corresponding group of cells exposed at 4°C. **, significantly different ($p < 0.05$) from the means of all other corresponding groups of cells. + or ++, significantly ($p < 0.05$) from the mean for the same treatment group at previous time points.

Figure 3.
Saturation kinetics of the transport of inorganic mercury (Hg^{2+}) as a conjugate of cysteine (Cys-*S*-Hg-*S*-Cys) or homocysteine (Hcy-*S*-Hg-*S*-Hcy) in ARPE-19 cells. Cells were exposed to 5 μM Cys-*S*-Hg-*S*-Cys (A) or Hcy-*S*-Hg-*S*-Hcy (B) in the presence of unlabeled Cys-*S*-Hg-*S*-Cys or Hcy-*S*-Hg-*S*-Hcy, respectively, for 30 min at 37°C and 4°C. Uptake was measured in the presence of NaCl or N-methyl-D-glucamine (NMDG). Curves were obtained using nonlinear regression analyses with the Michaelis-Menten equation: $y = ax/(b+x)$. Panel A: NaCl: $y = 111x/(160 + x)$, $r^2 = 0.995$. NMDG: $y = 24.8x/(195.0 + x)$, $r^2 = 0.989$. Panel B: NaCl: $y = 85x/(78 + x)$ $r^2 = 0.995$. NMDG: $y = 21x/(48 + x)$ $r^2 = 0.937$. Results are presented as means ± standard error. Data represent two experiments performed in triplicate. *, significantly

different (p < 0.05) from the mean for the corresponding group of cells exposed at 4°C. **, significantly different (p < 0.05) from the means of all other corresponding groups of cells. +, ++, +++, or ++++ significantly (p < 0.05) from the mean for the same treatment group at previous concentrations.
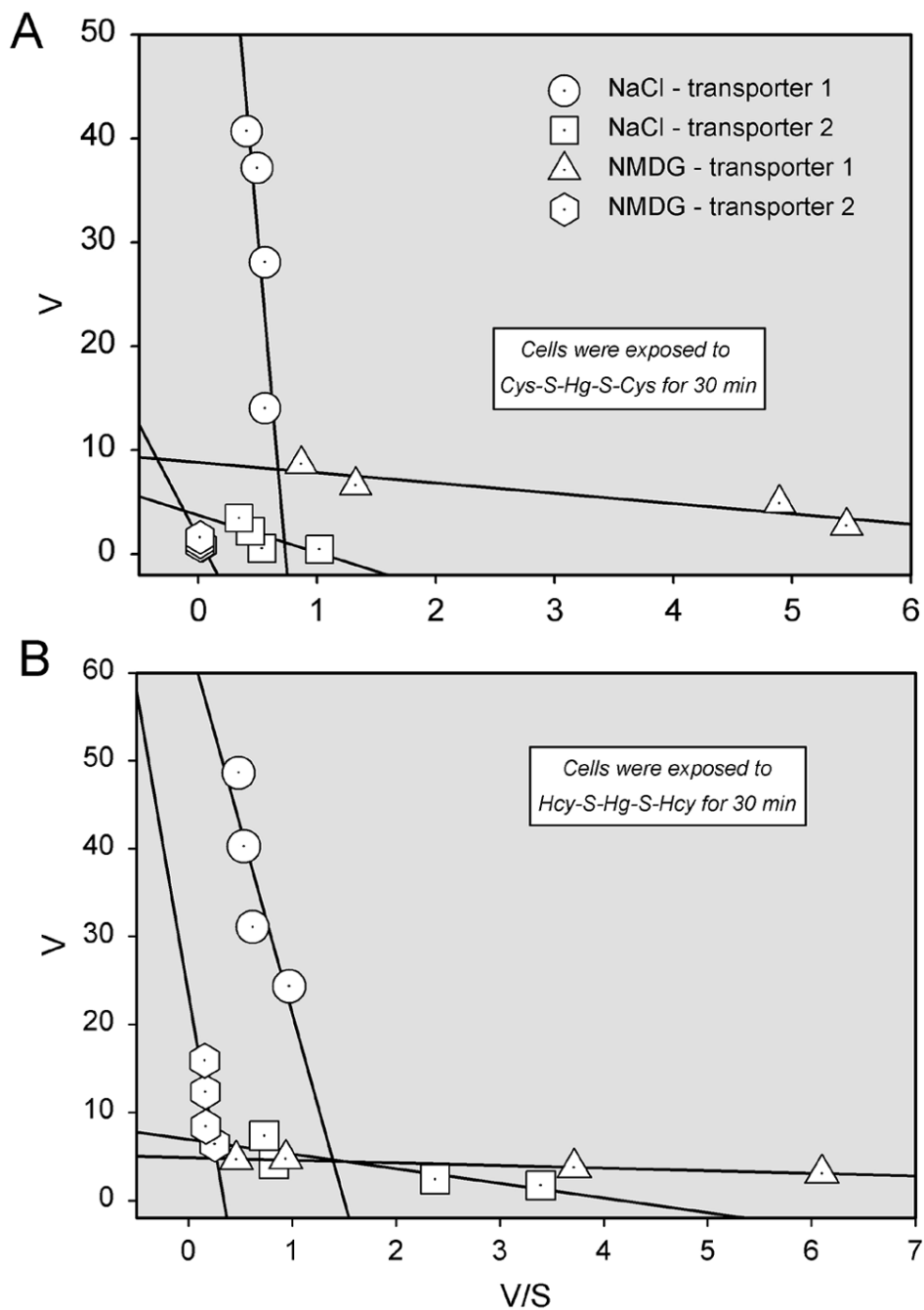
Figure 4.
Eadie-Hofstee plot derived from the examination of saturation kinetics of the transport of inorganic mercury (Hg^{2+}) as a conjugate of cysteine (Cys-*S*-Hg-*S*-Cys) (A) or homocysteine (Hcy-*S*-Hg-*S*-Hcy) (B) in ARPE-19 cells at 37°C. Linear regression analyses were used to generate lines with the following formula: y = ax + b. Panel A: NaCl (filled circles): y = 96.93 – 132.2x, $r^2 = 0.66$; NaCl (filled triangles): y = 3.72 - 3.5x, $r^2 = 0.55$. NMDG (open triangles): y = 8.82 – 0.99x, $r^2 = 0.86$; NMDG (open circles) y = 1.56 – 21.83x, $r^2 = 0.28$. Panel B: NaCl (filled circles): y = 63.99 – 42.67x, $r^2 = 0.781$; NaCl (filled triangles): y = 6.92 – 1.66x, $r^2 = 0.726$; NMDG (open circles): y = 23.6 – 68.8x, $r^2 = 0.554$ NMDG (open triangles): y = 4.85 – 0.297x, $r^2 = 0.987$ Results are presented as means ± standard error. Data represent two

experiments performed in triplicate. *, significantly different (p < 0.05) from the mean for the corresponding group of cells exposed to NMDG. +, ++, +++, or ++++ significantly (p < 0.05) from the mean for the same cell type at previous concentrations.
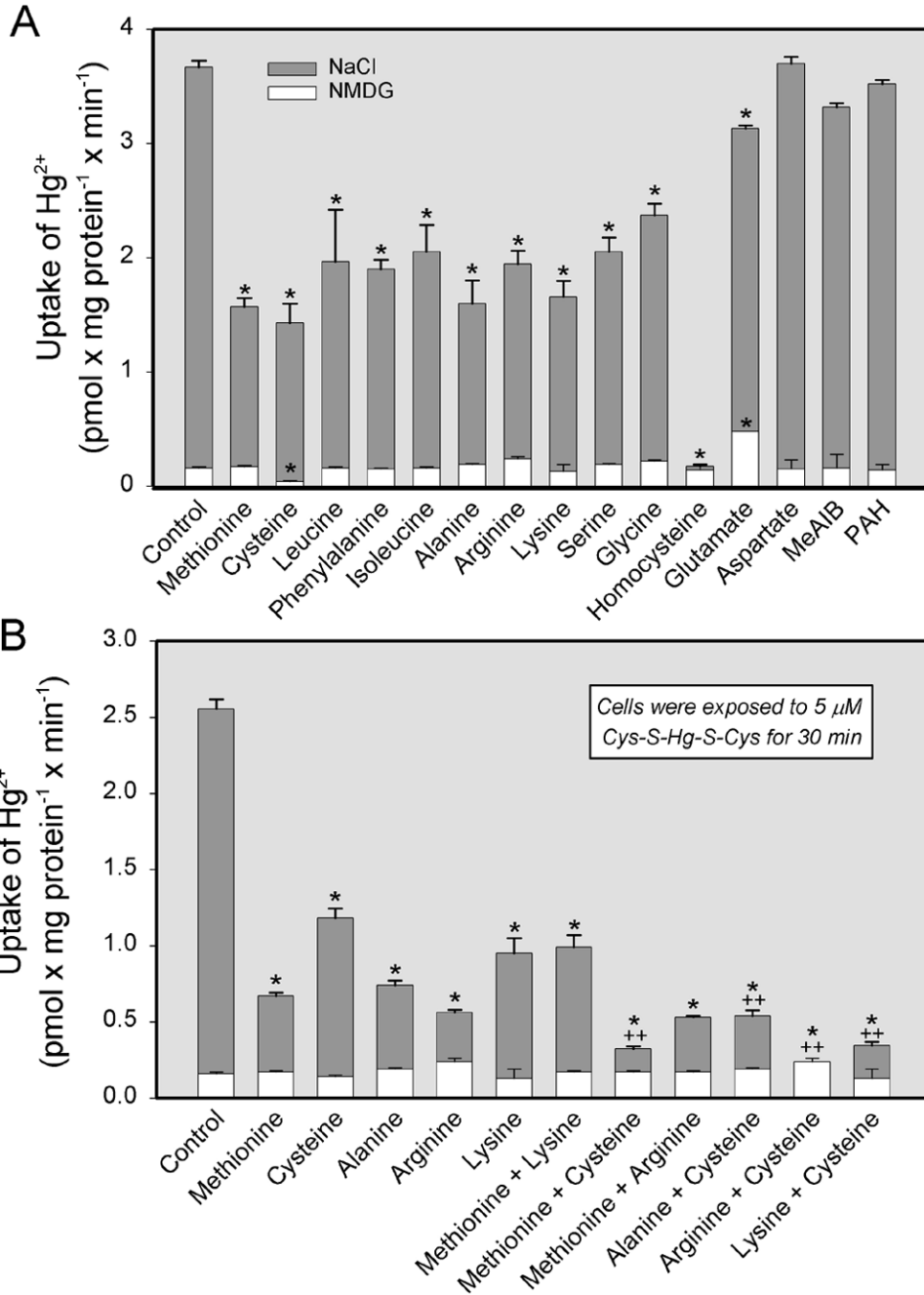
Figure 5.
Substrate specificity of the transport of inorganic mercury (Hg^{2+}) as a conjugate of cysteine (Cys-*S*-Hg-*S*-Cys) in ARPE-19 cells. Cells were exposed to 5 μM Cys-*S*-Hg-*S*-Cys for 30 min at 37°C in the presence of single amino acids (A) or in the presence of two amino acids (B) under Na^+-dependent or independent conditions. Each amino acid was used at a concentration of 3 mM. Results are presented as means ± standard error. Data represent two experiments performed in triplicate. *, significantly different ($p < 0.05$) from the mean for the control group of cells. ++, significantly ($p < 0.05$) from the mean for each of the two groups of cells exposed to the corresponding individual amino acids.
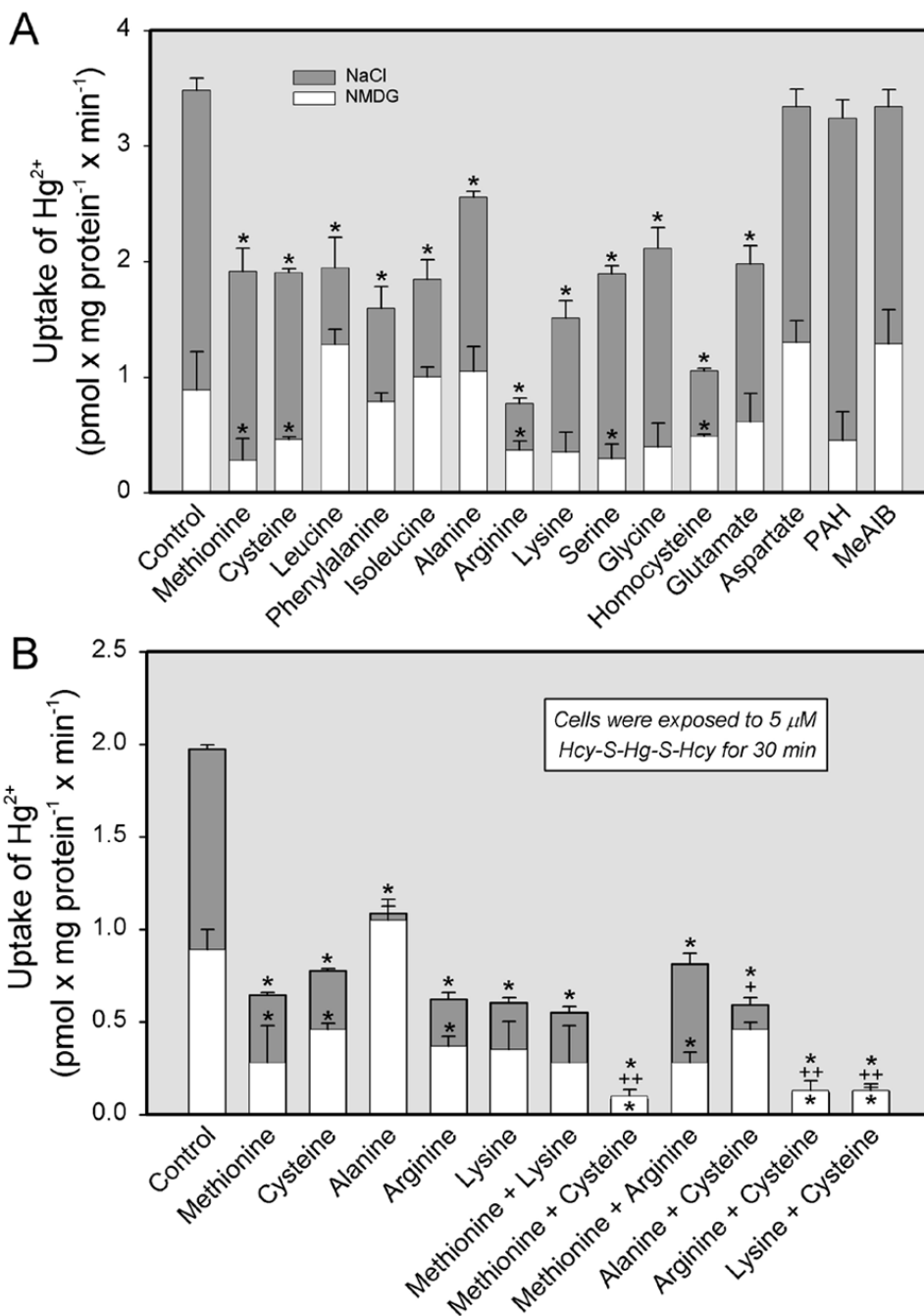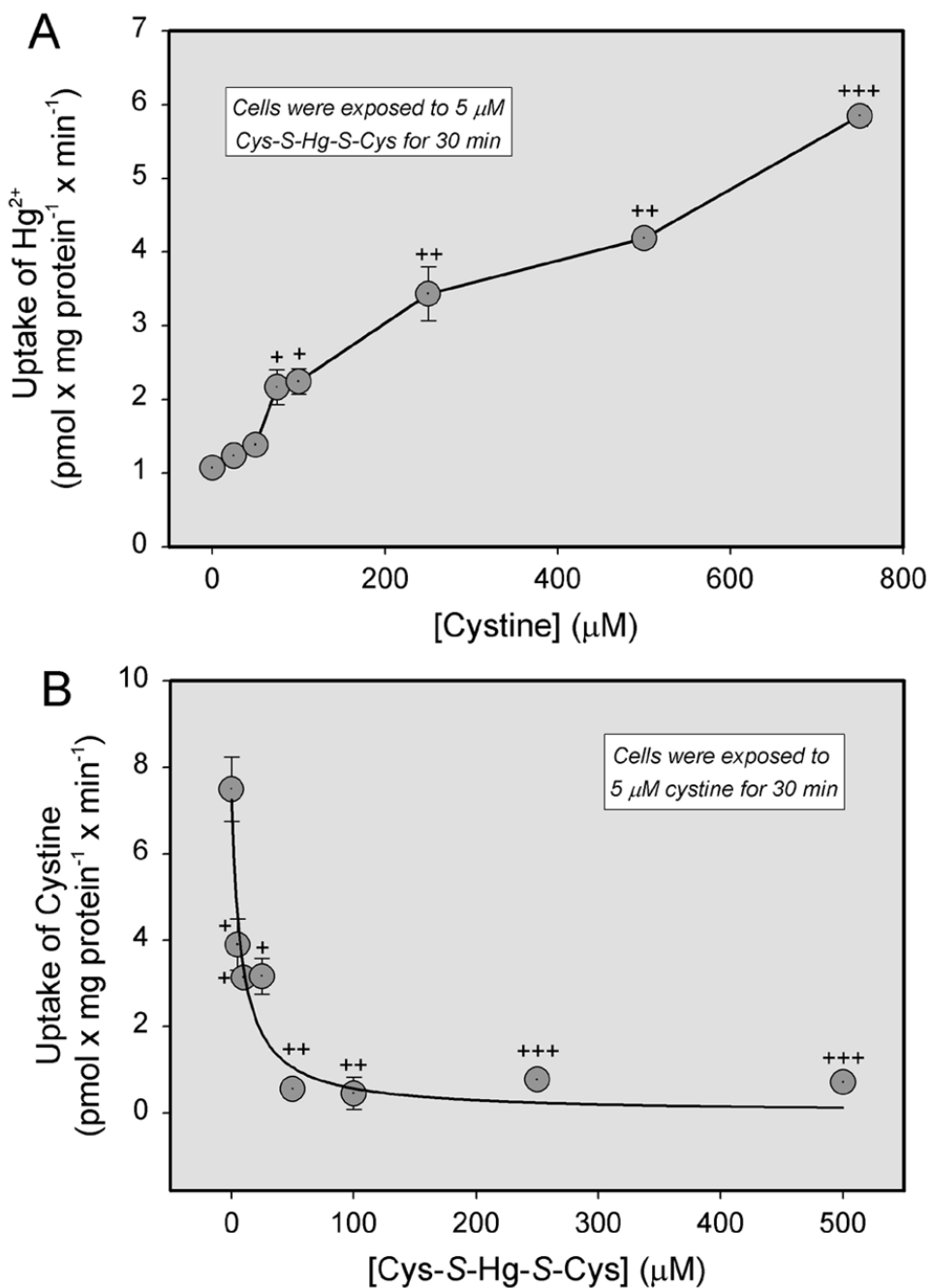
Figure 6.
Substrate specificity of the transport of inorganic mercury (Hg^{2+}) as a conjugate of homocysteine (Hcy-*S*-Hg-*S*-Hcy) in ARPE-19 cells. Cells were exposed to 5 μM Hcy-*S*-Hg-*S*-Hcy for 30 min at 37°C in the presence of single amino acids (A) or in the presence of two amino acids (B) under Na$^+$-dependent or independent conditions. Each amino acid was used at a concentration of 3 mM. Results are presented as means ± standard error. Data represent two experiments performed in triplicate. *, significantly different (p < 0.05) from the mean for the control group of cells. ++, significantly (p < 0.05) from the mean for each of the two groups of cells exposed to the corresponding individual amino acids.

Figure 7.
Uptake of inorganic mercury (Hg^{2+}) as a conjugate of cysteine (Cys-*S*-Hg-*S*-Cys) in the presence of unlabeled cystine (A), or uptake of cystine in the presence of unlabeled Cys-*S*-Hg-*S*-Cys (B). ARPE-19 cells were exposed to 5 μM Cys-*S*-Hg-*S*-Cys or cystine for 30 min at 37° C in the presence of NaCl. Results are presented as means ± standard error. Data represent two experiments performed in triplicate. +, ++, +++, significantly ($p < 0.05$) from the mean for the cells at the preceding concentration.
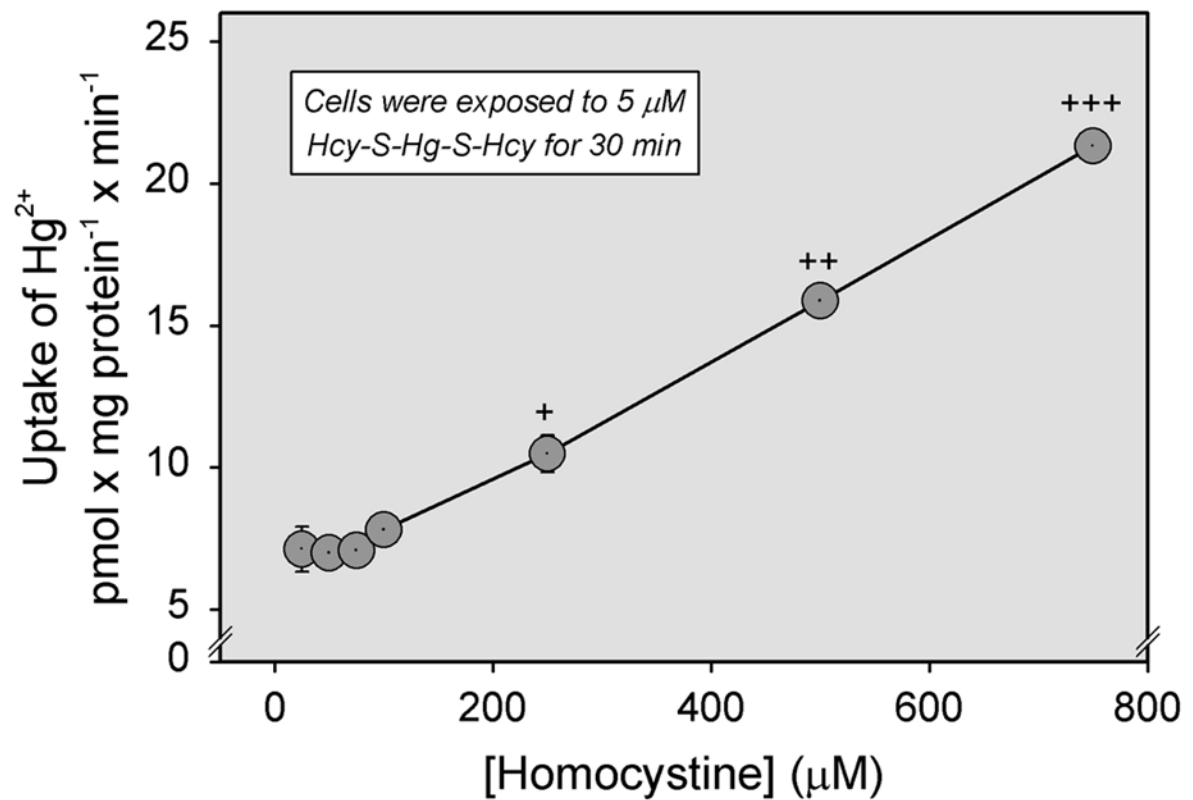
Figure 8.
Uptake of inorganic mercury (Hg^{2+}) as a conjugate of homocysteine (Hcy-*S*-Hg-*S*-Hcy) in the presence of unlabeled homocystine. ARPE-19 cells were exposed to 5 µM Hcy-*S*-Hg-*S*-Hcy for 30 min at 37°C in the presence of NaCl. Results are presented as means ± standard error. Data represent two experiments performed in triplicate. +, ++, +++, significantly ($p < 0.05$) from the mean for cells of the same treatment group at the preceding concentration.
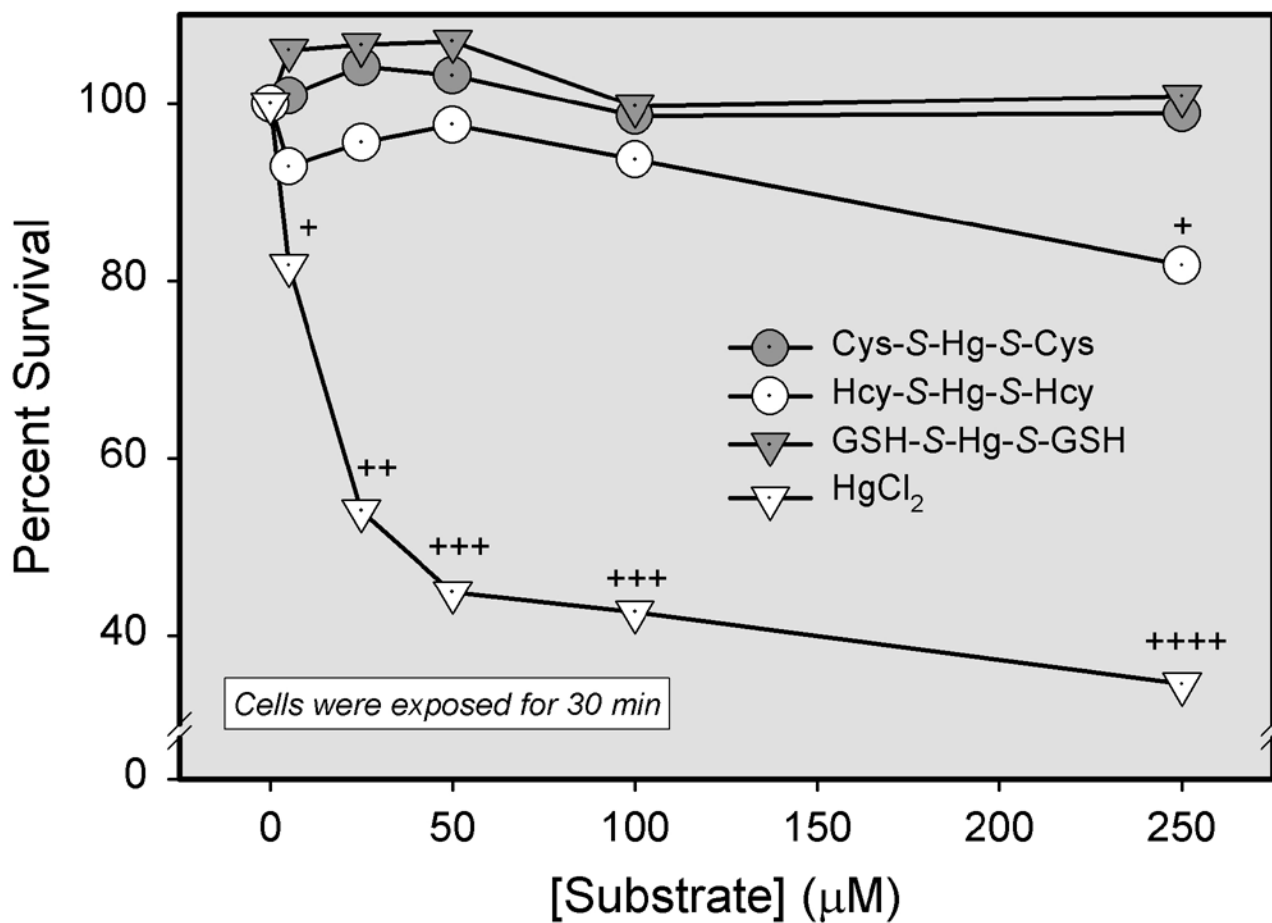
Figure 9.
Analyses of cellular viability following exposure of ARPE-19 cells to inorganic mercury
(Hg^{2+}) as a conjugate of cysteine (Cys-*S*-Hg-*S*-Cys), homocysteine (Hcy-*S*-Hg-*S*-Hcy),
glutathione (GSH-*S*-Hg-*S*-GSH) or $HgCl_2$. Cells were exposed to various concentrations of
each conjugate for 30 min at 37°C. Results are presented as means ± standard error. Data
represent two experiments performed in quadruplicate. +, ++, +++, or ++++, significantly (p
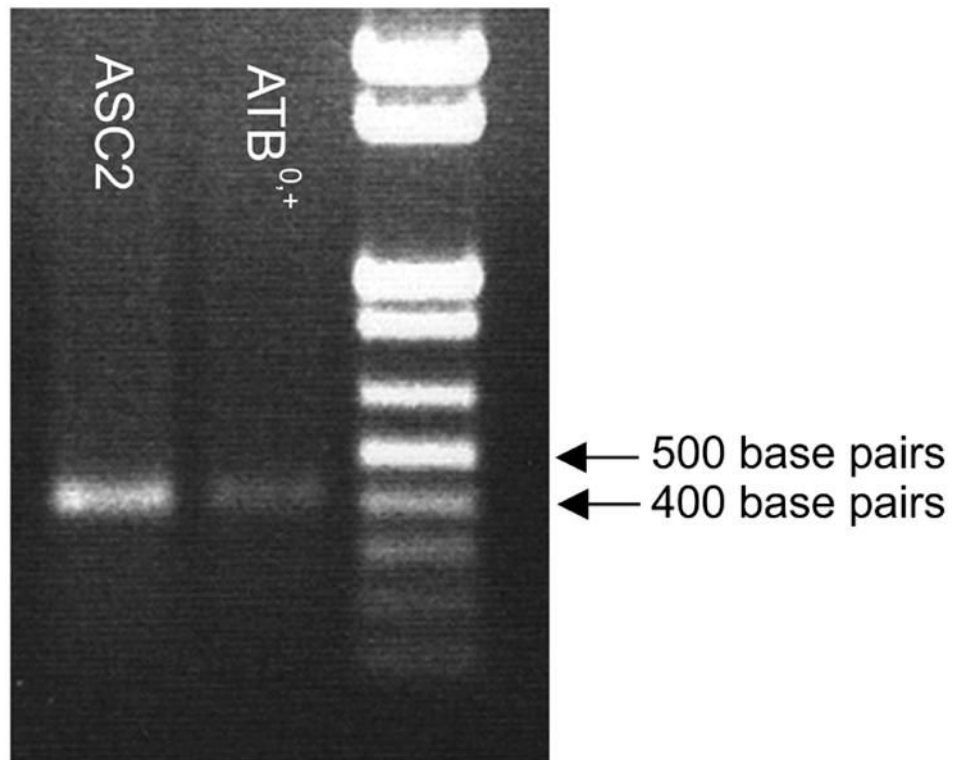< 0.05) from the mean for cells of the same treatment group at the preceding concentration.

Figure 10.
Agarose gel showing RT-PCR analyses of the expression of steady-state mRNA encoding
$ATB^{0,+}$ and ASC2 in ARPE-19 cells. The expected sizes of the RT-PCR products, as predicted
from the position of the primers, were 425 base pairs (bp) for system $B^{0,+}$ and 405 bp for system
ASC. Lane 1, system ASC; Lane 2, system $B^{0,+}$; Lane 3, DNA ladder.